JSAE 20159328
SAE 2015-01-1859

# Optimization of Mixture Formation and Combustion in Two-stroke OP Engine Using Innovative Diesel Spray Combustion Model and Fuel System Simulation Software.

**Leonid Grekhov**
Bauman Moscow State Technical Univ.

**Khamid Mahkamov, Andrey Kuleshov**
Northumbria Univ., Newcastle-upon-Tyne



## ABSTRACT

In this study theoretical investigations were carried out to determine design and working parameters modifications in order to increase by 20% power output and reduce fuel consumption in a marine two stroke medium speed diesel engine with opposite pistons. To achieve the above aim software packages, such as DIESEL-RK, INJECT and ANSYS, were deployed.

The phenomenological multi-zone fuel spray combustion model in DIESEL RK software was refined to take into account complex interactions of fuel sprays and the influence of air swirl in the cylinder on evolution of fuel spays. For this purposes a 3D grid was created with regular cubical cells in the combustion chamber of the engine. The density of mesh was 50 cells across the diameter of the cylinder. In contrast to CFD technique, the transfer of liquid fuel and fuel vapour in the computational grid was carried out using empirical equations which had been validated by other researchers. Such novel approach made it possible to preserve the high speed computational performance of DIESEL-RK and good accuracy of modeling. In this new methodology for calculation of combustion in multiple zones only energy balance equation is solved to calculate the temperature of combustion gases, fuel droplets and process of fuel evaporation. Computational time for modeling of one mode of engine's operation takes only few minutes even for the case when 8 side injectors are deployed in the cylinder. For optimisation of angles of sprays orientation a sub-programme is developed in C++ for 3D visualisation of modelling results using the cross platform library OpenGL. With refined model of combustion DIESEL-RK was further developed to make it possible to simulate simultaneous application of several separate fuel injection systems even with supply of different types of fuel into the cylinder. Optimisation of the engine also results in specification of requirements to fuel supply systems. Using such technical specification of requirements and using INJECT software the main design features of the main elements of the high pressure pump, pipe work of the fuel supply system and fuel injector are defined. It was found that the fuel injection pressure should be higher than 2000 bar but lower than 2800 bar so the Common Rail fuel supply system does not have advantages over conventional unit pump systems if no ultra-low limits on the level of emissions are imposed. Finally, the thermal loading of the engine's piston was evaluated using ANSYS software. It was found that the maximum temperature on edges of the piston's crown made of cast iron limits the level of enhancing of engine's performance.

## INTRODUCTION

Two-stroke opposed piston (OP) diesel engines have retained their relevance in some special applications due to their structural reliability, high power density and efficiency (42...45%) [1]. These engines are inferior to four-stroke engines in terms of particulate emission levels. This is due to the loss of lubricating oil from the surface of piston rings when pistons pass by the ports in the cylinder liner. However, the OP engines are well balanced and have low specific mass and dimensional parameters and therefore they are attractive alternatives for use in compact power plants, generators, ships, aircrafts and military vehicles. For example, the 6TD engine, shown in Fig. 1, has a capacity to produce the power output of 1007 kW with the engine volume being about 1 $m^3$ [2, 3].

To reduce the level of emissions of such engines it is necessary to use ERG, SCR, diesel particulate filters and other modern technical solutions (the modern fuel system, the effective piston rings, etc). For the above reasons, the development of new high performance engines or modernization of existing OP engines is a serious engineering challenge.

***Figure 1. Compact 6TD diesel produced by Kharkiv Malyshev Factory in Ukraine***

The aim of the current study is theoretical studies for optimization of design and operational parameters of the medium speed marine OP diesel engine 88-G in order to improve the engine fuel efficiency and increase its power output. The engine's technical specification is presented in Table 1 and its cross cut is shown in Fig. 2 [4].

***Table 1. Specification of the medium speed marine OP 88-G diesel engine***

| Parameter | Value |
|---|---|
| Bore | 230 mm |
| Stroke | 2 x 300 mm |
| Number of cylinders | 18 |
| Number of crank shafts | 4 |
| Angular offset of shafts | $9^0$ |
| Compression ratio | 19.5 |
| Max. cylinder pressure | 135 bar |
| Boost | Mechanic. assisted TC |
| Nominal power | 5152 kW @ 800 RPM |
| Maximum power | 6710 kW @ 900 RPM |
| Dimensions L x W x H | 7270 x 1920 x 3220 mm |

The engine has a side fuel injection system with two injectors supplying fuel into the combustion chamber through special grooves, made in the piston's crown with the angle between equal to $120^o$ (for convenience in servicing the injectors), see Fig. 3.

Each injector has 3 nozzles with diameters of 0.6 and 0.45 mm, with the smaller nozzle being directed along the clockwise air swirl, see Table 2 (shown in yellow).

At present CFD methods can be used for modelling of fuel/air mixing and combustion as a part of thermodynamic calculation of the whole working cycle of the engine. To reduce computational time required in certain cases it is possible to carry out CFD modelling for a section of the combustion chamber in which evolution of the fuel spray takes place but even in such simplified case significant computational resources and time (several hours) are needed to complete simulations. In engines with side fuel injection systems it is necessary to build the full 3D CFD model of the physical domain to describe evolution of all fuel sprays. The computational time required for such full 3D CFD simulations so substantial that it makes it unfeasible and in many cases impossible to use such the approach for solving optimisation problems with a large number of variables.

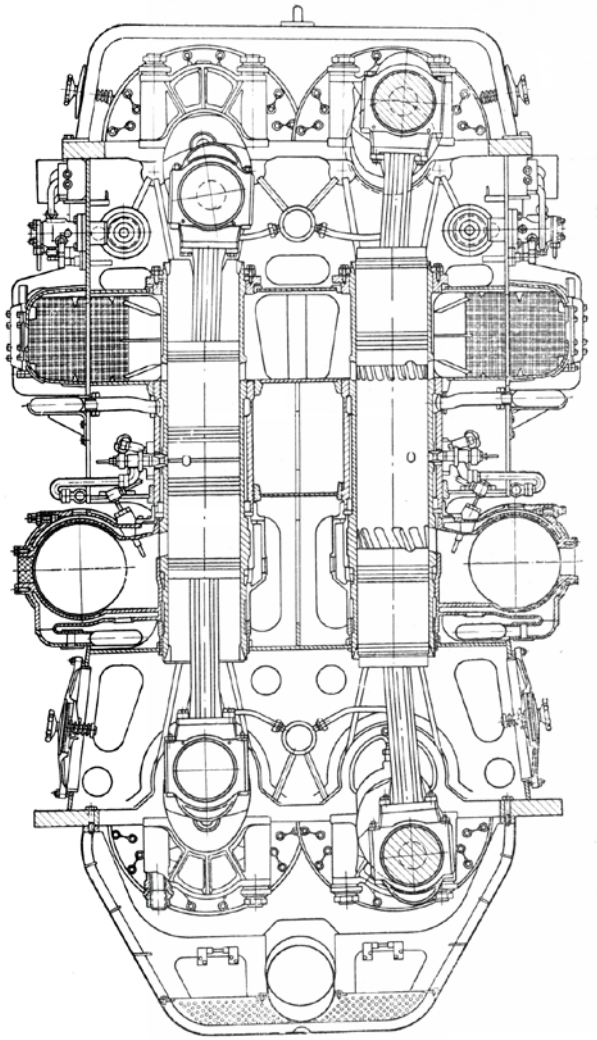

***Figure 2. Medium speed marine OP 88-G diesel engine.***

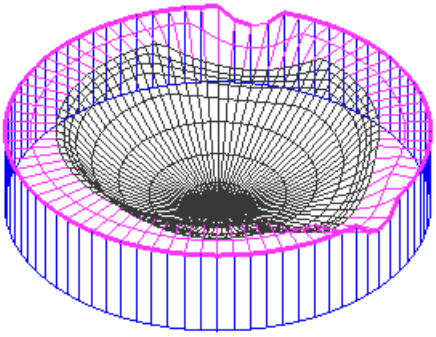

***Figure 3. The schematic of the piston's crown with grooves for the injectors in the OP 88-G diesel engine.***

***Table 2. Specification of the original injectors***

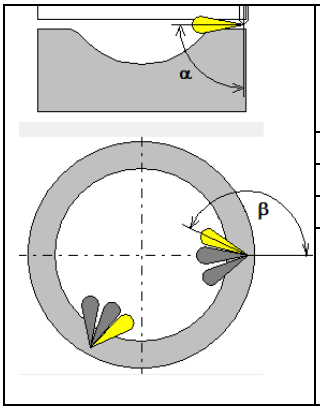


| Nozzles | Bore [mm] | α [deg] | β [deg] |
|---|---|---|---|
| 1 | 0.45 | 90 | 155 |
| 2 | 0.6 | 72.5 | 180 |
| 3 | 0.6 | 90 | -150 |

To make it possible to complete the engine optimisation in acceptable time, alternative approach can be deployed in which rapid phenomenological mathematical model of fuel/air mixing and combustion is used which takes into account interaction of fuel sprays in the combustion chamber of complex geometry and properties of various fuels.

In this work such the method is proposed based on using phenomenological model of multi-zone fuel spray and its combustion in diesel engine augmented by 3D characterization of the geometry of fuel spray characteristic zones to more accurately define the volumes of individual spay intersection zones and effect of the air swirl. The mathematical model is enhanced by 3D visualization program to graphically depict the spatial evolution of fuel sprays and interaction of individual fuel sprays in time to assist in selection of position of fuel injectors and determine diameters of their individual nozzles.

The theoretical investigations in this current research were performed using following software:

- DIESEL-RK [4 - 6] – full cycle engine simulation software for optimization of engine working parameters, gas exchange process, mixture formation and combustion;
- INJECT [14] – hydrodynamic fuel supply system simulation tool for analysis and optimization of the fuel injection systems;
- ANSYS – analysis of the thermal loadings of the engine piston.

## MODIFICATIONS OF COMBUSTION MODEL IN DIESEL-RK

Previously developed full cycle engine simulation software DIESEL-RK has been used for simulation of the engine working processes in this research. The combustion model of DIESEL-RK has the capacity:

- To provide the detailed description of the fuel sprays evolution process;
- To take into account the interactions of sprays with in-cylinder swirl and walls of the combustion chamber;
- To describe evolution of a Near Wall Flow (NWF) formed as a result of the spray/wall impingement. The shape of the NWF is a function of the impingement angle and the local swirl velocity;
- To describe interactions of the Near Wall Flows formed by adjacent sprays;
- To predict the evaporation rate in the different spray and NWF zones depending on the gas and wall temperatures.

In the model each fuel spray is split into a number of specific zones (see Fig. 4) in which different evaporation conditions exist.

Prior to the jet impingement, only the following three zones are considered in the spray:

1. The dense conical core;
2. The dense forward front;
3. The dilute outer sleeve.

The NWF which is formed as a result of the spray/wall impingement is inhomogeneous in the structure, density and temperature, which makes the calculation of the fuel evaporation proves very difficult. It is therefore convenient to split the NWF into several zones with the averaged heat and mass transfer coefficients. This split is made similarly to the free spray's split into characteristic zones. After the impingement takes place, the following new zones are considered:

4. The axial conical core of the NWF;
5. The dense core of the NWF on the piston bowl surface;
6. The dense forward front of the NWF;
7. The dilute outer zone of the NWF.

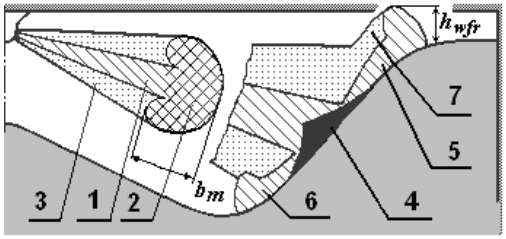


***Figure 4. Characteristic zones of the diesel spray***

Zones, formed on the cylinder liner surface and on the cylinder head, are also taken into account. The piston bowl in the modeling process is assumed to have an arbitrary axysymmetric shape. The combustion model supports central, non-central and side fuel injection systems.

To make possible an optimization of the multiple injection strategy (including the PCCI concept) the combustion model includes the Low Temperature Combustion technique [6] and predicts the self ignition delay by means of detail chemistry simulation [7]. The pre-calculated comprehensive 4-D map of ignition delay periods is used. This 4-D map is developed using CHEMKIN detailed chemistry simulations and takes into account effects of the temperature, pressure, Fuel/Air ratio and EGR on the ignition delay period. The phenomenological soot formation/oxidation sub-model takes into account the distribution of the droplet SMD during the injection process and specifics of the heat release.

DIESEL-RK supports the use of Venturi nozzle to mix the exhaust gases prior to entering the gas turbine with air after its cooled for the case when the boost pressure slightly exceeds the inlet pressure of the turbine.

DIESEL-RK has been previously validated using published and provided by manufacturers experimental data obtained on high-, medium- and low speed engines. The results of simulations of two-stroke engines with side injection systems such as OP locomotive 10D100 and marine g Mitsubishi UEC45LA engine with uniflow scavenging were published in [8, 9]. Comparison of results demonstrates a good agreement between theoretical and experimental sets of data.

In two stroke engines with side fuel injection systems there is a significant deformation of the geometry of free fuel sprays caused by a swirl. Unlike four-stroke engine, the fuel sprays in two stroke engines might intersect with each other in the volume of the combustion chamber. The temperature in the intersection zones might be lower than the temperature in the "parent" zone and the evaporation rate and combustion rate will decrease. To account for this phenomena the existing fuel spray combustion model was refined

as follows:

- 3D characterization of the geometry of zones is implemented which makes it possible to more accurately define the volume of spay intersection zones;
- The temperatures in the characteristic zones are calculated using more detailed energy balance equations.
- The equilibrium temperatures of fuel droplets in the evaporation model are calculated using equations describing the heat balance around droplets.
- The 3D fuel spray visualization tool is included for optimization of nozzle directions and minimization of spatial spray interactions.

## CALCULATION OF EQUILIBRIUM TEMPERATURE OF INJECTED FUEL DROPLETS

Accurate calculation of the evaporation rate of fuel droplets during fuel/air mixing and combustion processes is of a paramount importance in modelling engines since the fuel evaporation rate determines the heat release dynamics during combustion [6, 10].
The rate of the change in the diameter of the fuel droplets prior and after ignition is defined using the equation by B.I. Sreznevskiy:

$$d_k^2 = d_0^2 - K\,\tau_u \qquad (1)$$

where $d_0$ and $d_k$ are the initial and current diameters of the droplet, respectively; $K$ is the evaporation constant, $\tau_u$ is the time elapsed from the instance when the droplet entered the corresponding characteristic zone. Modern fuel injection systems provide a high uniformity in atomisation of fuel and therefore calculations of the fuel droplets evaporation rate can be carried out using the value of the Sauter Mean Diameter of the droplet $d_{32}$. It is assumed in calculations that $d_0 = d_{32}$.

The Sauter Mean Diameter $d_{32}$ of droplets is calculated using the dimensionless parameters [11] as follows:

$$d_{32} = 1.7\, d_n\, M^{0.0733} \left(\rho We\right)^{-0.266}, \qquad (2)$$

where $We = U_{0m}^2\, d_n\, \rho_f / \sigma_f$ , (3)

$$M = \mu_f^2 / \left(\rho_f\, d_n\, \sigma_f\right), \qquad (4)$$

$$\rho = \rho_{air} / \rho_f \; ; \qquad (5)$$

Here $d_n$ is the diameter of injector nozzles [m]; *We* – Weber's number which is the ratio of the inertial force and surface tension; $M$ is the squared Ohnesorge number, the parameter defined by the ratio of forces due to the surface tension, inertia and viscosity; $\rho$ is the ratio of the air density $\rho_{air}$ in the cylinder and fuel density $\rho_f$, $U_{om}$ is the velocity of fuel in the nozzle exit [m/s], $\sigma_f$ is surface tension factor of fuel [N/m] and $\mu_f$ is the fuel dynamic viscosity coefficient [Pa s].

The evaporation constant $K_i$ is calculated for each characteristic zone $i$ as

$$K_i = 4 \cdot 10^6\, Nu_{Di}\, D_{pi}\, p_{Si} / \rho_f \; , \qquad (6)$$

where $Nu_{Di}$ is the Nusselt's number for the diffusion process or the Sherwood's number *Sh* in the individual zone [6]; $D_{pi}$ is the baro-diffusion coefficient for the individual zone:

$$D_{pi} = D_{po} \left(T_{ki} / T_o\right)\left(p_o / p\right). \qquad (7)$$

The baro-diffusion coefficient $D_{pi}$ depends on the equilibrium temperature of the droplet $T_{ki}$ and current in-cylinder pressure $p$. In Eq. (6) $p_{Si}$ is the saturated vapor pressure at the temperature $T_{ki}$ for the individual zone; $D_{po}$ is the baro-diffusion factor determined for atmospheric conditions [$p_o$, $T_o$].

The baro-diffusion factor $D_{po}$ is calculated as

$$D_{p0} = \frac{D_{C0}}{R_{vap}\, T_0} \; , \qquad (8)$$

where $D_{co}$ is the coefficient of concentration diffusion [m$^2$/s]; $R_{vap}$ is the specific gas constant for fuel vapour [J/(kg K)] and $T_o$ = 273 K.

$$R_{vap} = \frac{R}{\mu}, \qquad (9)$$

where $\mu$ is the molecular mass of fuel [kg/kmol], $R$ is the universal gas constant equal to 8310 J/(kmol K).

The vapour saturation pressure can be determined from Clausius - Clapeyron equation:

$$p_S = \exp\left(A - B / T_{ki}\right), \qquad (10)$$

where $T_{ki}$ is equilibrium temperature of the droplet.

Coefficients $A$ and $B$ in Eq. (10) are determined using two sets of known values of the saturated pressure and temperature:

$$B = \frac{\ln(p_{Scr}) - \ln(p_{S1})}{\frac{1}{T_1} - \frac{1}{T_{cr}}}; \quad A = \ln(p_{S1}) + \frac{B}{T_1}. \qquad (11)$$

Here $p_{S1}$ is the saturated vapour pressure at some low temperature $T_1$ and $p_{Scr}$ is the saturated vapour pressure at the critical temperature $T_{cr}$.

The equilibrium temperature of the droplet $T_{ki}$ is determined using the equation of the energy balance between the heat delivered to the droplet from ambient gas due to the heat conductivity and the heat consumed during heating of liquid fuel, its evaporation and superheating of vapour to the temperature $T_{ki}$.

The fuel temperature in the centre of the droplet is assumed be equal to the surface temperature $T_{ki}$. The energy balance equation for this case is proposed by D.N. Vyrubov [12]:

$$\lambda_a \left(T_i - T_{ki}\right) = D_{pi}\, p_{Si} \left[ C_f \left(T_{ki} - T_f\right) + h_{evap} + C_{fv} \frac{T_i - T_{ki}}{2} \right] \qquad (12)$$

where $T_i$ is the temperature in the characteristic zone [K]; $\lambda_\alpha$ is the coefficient of the heat conductivity in air for the current temperature and pressure in the cylinder [W/(m K)]; $C_f$ is the heat capacity of fuel [J/(kg K)]; $T_f$ is the initial temperature of fuel [K]; $h_{evap}$ is the enthalpy of evaporation of fuel [J/kg] and $C_{fv}$ is the heat capacity of fuel vapour [J/(kg K)]. In Eq. (12) the values of $p_{Si}$ and $\lambda_\alpha$ depend on $T_{ki}$. Physical and chemical properties of diesel fuel used in calculations are presented in Table 3.

Fig. 5 shows results of calculation of the equilibrium droplet temperature of diesel fuel and methanol as a function of the temperature in the dilute outer characteristic zone of the fuel spray. The results of calculation for methanol are presented to illustrate effect of fuel properties on parameters of evaporation.

Fig. 6 presents results of calculation of the duration of full evaporation of fuel droplets with diameter of 10 μm as a function of the temperature $T_i$ in the dilute outer characteristic zone of the fuel spray. For calculation of the evaporation constant $K_i$ the value of $Nu_D$

equal to 20 was used in accordance with recommendations in [10, 12].

***Table 3. Physical and chemical properties of diesel oil and methanol***

| Properties | Diesel oil | Methanol |
|---|---|---|
| Mass fraction of C in the fuel | 0.87 | 0.374 |
| Mass fraction of H in the fuel | 0.126 | 0.125 |
| Mass fraction of O in the fuel | 0.004 | 0.499 |
| Low heating value $H_u$ , MJ/kg | 42.5 | 19.9 |
| Density of fuel $\rho_f$ at 323 K, kg/m$^3$ | 830 | 791.7 |
| Surface tension factor $\sigma_f$ , N/m | 0.028 | 0.022 |
| Dynamic viscosity $\mu_f$ , Pa·s | 0.003 | 0.0006 |
| Enthalpy of evaporation $h_{evap}$ , kJ/kg | 250 | 1173 |
| Liquid fuel heat capacity $C_f$ , J/kg K | 1853 | 2510 |
| Fuel vapor heat capacity $C_{fv}$ , J/kg K | 2223 | 1257 |
| Molar mass of fuel $\mu$, kg/kmol | 190 | 32.04 |
| Diffusion factor $D_{c0}$ at atmospheric conditions, m$^2$/s | 3.7 10$^{-6}$ | 1.5 10$^{-5}$ |
| Temperature $T_1$ , K (Eq. 11) | 480 | 293 |
| Saturated vapor pressure at $T_1$ , MPa | 0.0477 | 0.0276 |
| Critical temperature $T_{cr}$ , K | 710 | 513 |
| Saturated vapor pressure at $T_{cr}$ , MPa | 1.616 | 7.98 |

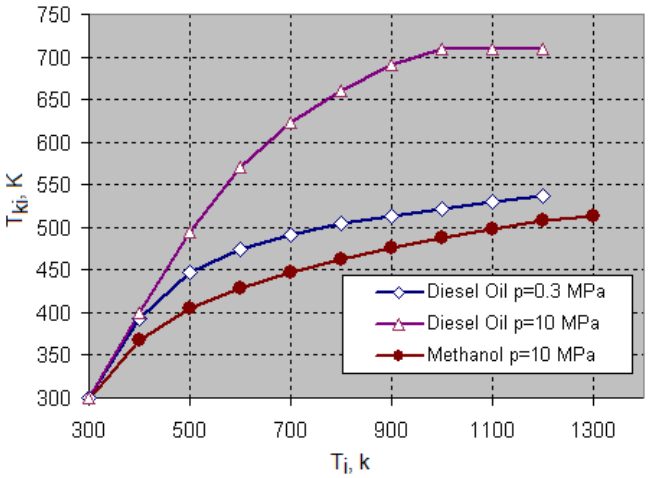


***Figure 5. The equilibrium temperature of droplets $T_{ki}$ for diesel oil and methanol as a function of the temperature $T_i$ in the dilute outer characteristic zone of the fuel spray.***

It can be seen in Fig. 5 that the equilibrium droplet temperature $T_{ki}$. Considerably changes during the cycle and using its average value during simulations may result in production of a considerable error in estimating the amount of evaporated fuel during the ignition delay period. During the combustion process at high pressures (more than 100 bar) the value of the equilibrium temperature of droplet corresponding to the critical temperature should be used but in the relatively "cold" characteristic zones such as the dense free spray core and dense core of NWF the temperatures are significantly lower and therefore Eq. (12) should be used for determination of $T_{ki}$..

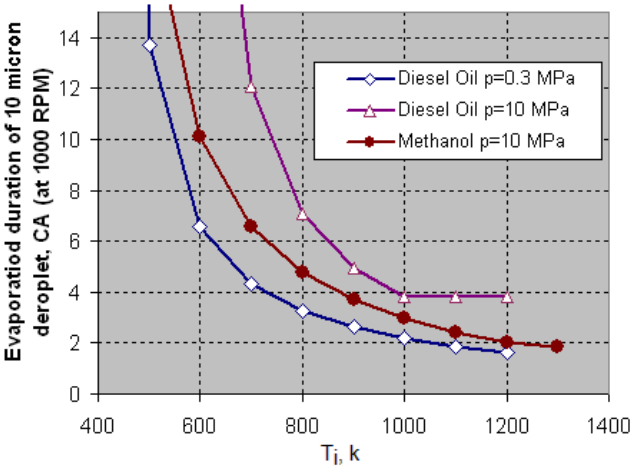


***Figure 6. Duration of full evaporation of fuel droplets with the diameter of 10 μm as a function of the temperature $T_i$ in the dilute outer characteristic zone of the fuel spray (in CA deg. for the engine speed of 1000 RPM)***

The rate of the fuel evaporation is calculated separately for every EFM and for every time step a decrease in the diameter of the fuel droplets is defined. Such procedure makes it possible to account for the influence of features in the fuel injection profile on the evaporation intensity and to estimate with a high accuracy the amount of fuel evaporated during the ignition delay and burnt in accordance with the volumetric mechanism.

For the late combustion phase (following the termination of the fuel injection) the duration of afterburning is determined by the time $\tau_{i.burn}$ which is necessary for evaporation and combustion of large fuel droplets formed at the end of the injection process [6, 10]. The characteristic diameter of these large droplets $d_l$ is calculated using Eqs. (1) and (2) assuming that $U_{om}$ is the average injection velocity of the last 5% of the fuel injected and $d_l = d_{32}$ is characteristic SMD of the large droplets in the last 5% of EFM's. The time $\tau_{i.burn}$ is calculated as:

$$\tau_{i\,burn} = d_l^2 \big/ K_u [1 + 2.5 \cdot 10^6 \; K_{ENV} / (\alpha - 1)] \quad (13)$$

where $K_u = Y\, K_{ENV}$; $K_{ENV}$ is the evaporation constant in the dilute outer surrounding of the spray, $\alpha$ is the Air/Fuel equivalence ratio in the cylinder. It is assumed that the large fuel droplets, which were formed at the end of injection with the spray velocity being slow, do not reach the walls and evaporate in the volume after the dense spray core is dissipated.

## 3D CHARACTERIZATION OF THE GEOMETRY OF ZONES AND THEIR TEMEPRATURE CALCULATIONS

In the combustion model in DIESEL-RK software a spray (deformed by swirl) is represented as a set of a cone and truncated cones with the apex of the cone being point of injection. The base of cones is an ellipse which is split into four unequal quarters [5-9] each characterized by dimensions $y_1$, $y_2$, $y_3$ *and* $y_4$, respectively, as shown in Fig. 7. Shifting of the spray and deformation of its shape by the air-flow in the cylinder are calculated using methodology described in [5-9] and depend on the local velocity of the swirl,

spray orientation, density of gas in the cylinder and mean diameter of droplets.

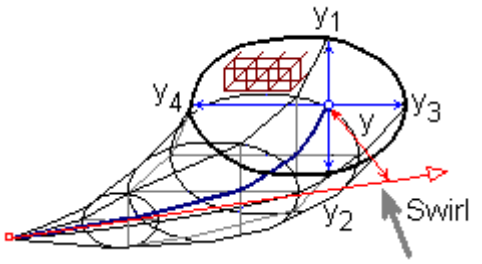


***Figure 7. Representation of the spray deformed by the swirl as a set of a cone and truncate cones***.

The shape of Near Wall Flow (NWF) is also assumed to have an ellipse shape which is divided into four unequal parts. The NWF is formed on the surface of the piston bowl and cylinder liner and its geometry is defined in a polar coordinates. This makes it possible to analytically calculate interactions of NWFs from adjacent sprays. Calculations for the set of cone and truncate cones are much more sophisticated.

To estimate the temperature in various zones of the spray it is necessary to calculate their volumes, especially in the core of the spray and in its front. Until the spray reaches the walls of the piston bowl or the cylinder liner the volumes of the spray zone can be calculated using the geometries in the set of cone and truncated cones into which the spray is split. But if spray/wall impingements take place or there is interaction between adjacent sprays it is necessary to deploy novel approach for evaluation of volumes in different zones. Additionally, in this work the engine is considered in which there are several fuel sprays evolving in the cylinder in different directions. Finally, the bowl in the piston has a very complex geometry. For accurate calculation of the spray zone volumes, the total space of the cylinder is split into regular grid with cubical cells. There are usually from 50 to 80 cells placed across the diameter of the cylinder. Every cell is assigned a marker, indicating the domain it belongs to, e.g. piston bowl, cylinder liner, zone of i-spray. By summing the volumes of cells with corresponding markers it is possible to accurately determine the volume of spray zones and define the locations and instances of time for interaction of fuel spray zones.

In parallel, such the 3D characterization of the geometry inside the cylinder makes it possible a spatial visualization of the sprays evolution. The visualization tool is developed in C++ using the cross platform library Open GL.

50 cells across diameter of the cylinder were used in this current research but the finer grid can be specified in the graphical user interface of DIESEL-RK.

The following assumptions were made to calculate temperatures in spray zones:

- There is an even distribution of temperature, fuel and its vapour inside each spay zone;
- Transfer of fuel and its vapour between spay zones is calculated using empirical equations proposed in [6];
- The spray front receives air from the cylinder volume whilst the spray core receives air from the spray's front;
- The gas in each zone is made of air and products of stoichiometric combustion. The current value of the heat capacity of such mixture depends on the temperature and composition of combustion products;
- The temperature in NWF is calculated using previously validated empirical equations as a function of temperature of walls and average temperature in the cylinder;
- Fuel droplets are heated up in zones in such a way that their initial temperature instantaneously rises to the equilibrium temperature of evaporation $T_k$ in the zone;
- All fuel droplets in the individual zones have the same diameter $d_{32}$ (Sauter Mean Diameter: SMD).
- Heat transfer is carried out only by convection of air, fuel and its vapour;
- The temperatures of air and fuel vapour are equal inside the individual zones.

In accordance with the above assumptions the temperature $T$ of zones in the core part and front of the spray are defined using the following energy balance equation:

$$\Delta U_a + \Delta U_f + \Delta U_{vf} = \Delta Q_a + \Delta Q_f + \Delta Q_{vf} - \\ - pdV - H_{evap} + \Delta Q_X \quad (14)$$

Here $\Delta U_a$ is the change of internal energy of air in the zone during the time step; $\Delta U_f$ is the change in the internal energy of liquid fuel during the time step $\tau$; $\Delta U_{vf}$ is the change in the internal energy of fuel vapour in the zone during the time step; $p\,dV = p\Delta V_C \frac{V_Z}{V_C}$ is work done by gas in the zone during the time step with $dV_C$ being the change of the cylinder volume and $V_Z$ being the volume of the zone; $\Delta Q_a = \Delta m_{aZ} C_{VaZ} T_Z$ is the heat transferred to the zone from another zone with the temperature $T_Z$ by the mass of air $\Delta m_{aZ}$ with the average heat capacity $C_{VaZ}$; $\Delta Q_f = \Delta m_{fZ} C_f T_{kZ}$ is the heat transferred to the zone from another zone by the mass of fluid fuel $\Delta m_{fZ}$ with temperature of $T_{kZ}$; $\Delta Q_{vf} = \Delta m_{vfZ} C_{vf} T_Z$ - is the heat transferred to the zone from another zone with the temperature $T_Z$ by the mass of fuel vapour $\Delta m_{vfZ}$ with the average heat capacity $C_{vf}$; $H_{evap} = \Delta m_{fe} h_{evap}$ is the enthalpy of evaporation of fuel in the zone with $h_{evap}$ being the specific enthalpy of evaporation of fuel; $\Delta Q_X = m_{vf2}\, \xi_b\, H_U$ is the heat released in the process of combustion of fuel during the time step with $\xi_b$ being the coefficient taking into account the fraction of burnt fuel vapour [5] and $H_u$ being the calorific value of fuel.

$$\Delta U_a = m_{a2} Cv_{a2} T_2 - m_{a1} Cv_{a1} T_1$$

where indices 1 and correspond to the beginning and end of time interval during the time step; $C_{Va}$ is the mass averaged constant volume heat capacity of air as a function of the temperature and composition of combustion products; $m_a$ is the mass of air in the zone.

$$m_{a2} = m_{a1} + \Delta V_Z \rho_Z + \Delta m_{vf\,x}$$

Here $\Delta V_z$ is the increase of the volume of the zone duet intake of air from the cylinder volume or other zones

(this increase is calculated by summing the volumes of cells in the zone during the time step); $\rho_z$ – is the density of air of the zone from which air flows in; $\Delta m_{vfx}$ – is the mass of burnt fuel vapour;

$$\Delta U_f = m_{f2} C_f T_{k2} - m_{f1} C_f T_{k1}$$

Here $C_f$ is the heat capacity of fluid fuel; $T_k$ – equilibrium temperature of fuel droplets (in the core of the spray new portions of injected fuel have the temperature equal to the temperature of fuel in the nozzle of the injector); $m_f$ is the mass of the fluid fuel in the zone.

$$m_{f2} = m_{f1} + \Delta m_{f\,inj} - \Delta m_{f\,d} - \Delta m_{f\,e}$$

where $\Delta m_{f\,inj}$ is the mass of fluid fuel injected by the injector or transferred from other zones during the time step; $\Delta m_{f\,d}$ is the mass of fluid fuel transferred from the individual zone to other adjacent zones; $\Delta m_{f\,e}$ is the mass of evaporated fluid fuel in the zone during the time step.

$$\Delta U_{vf} = m_{vf\,2} C_{vf} T_2 - m_{vf\,1} C_{vf} T_1$$

$C_{vf}$ is the heat capacity of the fuel vapour; $m_{vf}$ is the mass of the fuel vapour in the zone

$$(m_{vf\,2} = m_{vf\,1} + \Delta m_{vf\,s} - \Delta m_{vf\,d} + \Delta m_{f\,e} - \Delta m_{vf\,x});$$

Here $\Delta m_{vf\,s}$ is the mass of the fuel vapour transferred into the individual zone during the time step; $\Delta m_{vf\,d}$ is the mass of the fuel vapour transferred from the individual zone to adjacent zones.

The mass of evaporated fuel is calculated using diameters of fuel droplets prior and after evaporation:

$$\Delta m_{fe} = \left(m_{f1} + \Delta m_{f\,inj}\right)\left[1 - \left(\frac{d_{32\,2}}{d_{32\,mix}}\right)^3\right] \qquad (15)$$

In calculations it was assumed that first droplets mix and then evaporate. The diameter of the fuel droplets in the zone after their mixing is

$$d_{32\,mix} = \frac{N_1 d_{321}^3 + N_{inj} d_{32\,inj}^3}{N_1 d_{321}^2 + N_{inj} d_{32\,inj}^2}; \qquad (16)$$

where $N_1$ and $d_{32.1}$ is the number and Sauter Mean Diameter of droplets in fuel with mass of $m_{f1}$; $N_{inj}$ and $d_{32.inj}$ is the number and Sauter Mean Diameter of droplets in fuel with mass of $m_{f\,inj}$.

The diameter of droplets after evaporation is calculated using Eq. (1) presented as

$$d_{32\,2} = \sqrt{d_{32\,mix}^2 - K\tau}$$

where $K$ is the constant of evaporation computed in accordance with Eq. (6).

The temperature $T_2$ in the zone, diameter of droplets and amount of evaporated fuel are calculated using equations (1) - (16). Calculations in each zone are carried out with the time step corresponding to 0.25 degrees of CA. The computing time of the full engine cycle is about 3 min on a conventional PC, which is substantially faster (by factor of several hundred) than the case when CFD used for the similar task. Results of calculation of temperature and diameter of the fuel droplets in frontal zones of the three sprays in the engine under consideration are shown in Figure 8.

Previously developed fuel injection system hydrodynamic simulation software INJECT [14, 15] was used for the engine fuel system analysis and optimization. This software was used to calculate injection profiles for every engine's operation mode.

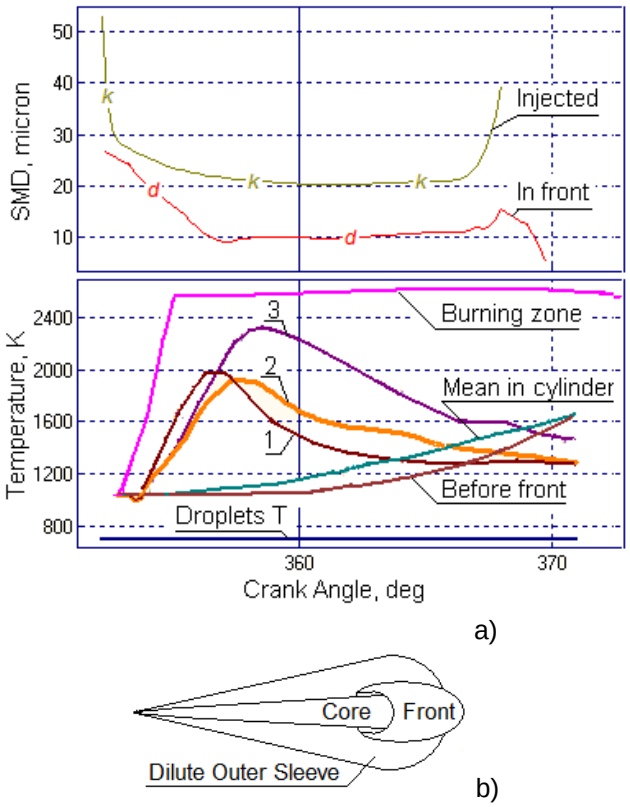


***Figure 8. a) The temperature and SMD in the frontal zones of three sprays (#1, #2, #3) in the combustion chamber of the engine under consideration - 8000 kW @ 900 RPM (120% of the original maximum power output); b) Scheme of fuel spray zones.***

## SIMULATION OF THE BASE CONFIGURATION OF THE ENGINE

To calibrate the mathematical model engine simulations were performed for the following operating modes: 5152 kW@ 800 RPM (77%); 5667 kW @ 800 RPM (84%) and 6710 kW @ 900 RPM (100%), see Table in Appendix A. The values of the pressure ratios for the compressor and turbine at the above operating modes are shown in Fig. 9. The difference between power required to drive the compressor and exerted by the turbine is compensated by the crank shaft drive of the compressor and accounted in simulation results.

Results of calculations of the effective flow area of intake and exhaust ports, the pressure in cylinder, intake and exhaust manifolds and the gas flow through intake and exhaust ports for the operating mode in which power output is 77% of the maximum value are presented in Fig. 10. The obtained theoretical results on the Heat Release Rate (HRR), Injection Profile, Spray Tip Penetration and SMD for the same operating mode are shown in Fig. 11. Graphical representation of the evolution of the sprays at this operating mode are presented in Fig. 12. Spray cores are shown in the different colors, fronts of all sprays are shown in brown, NWFs are in red and zones of spatial spray intersection are presented in black. Results of simulation of the above operating mode of the engine indicates that no fuel spay reaches the cylinder liner and there is a strong deformation of Spray # 3 which has a counter swirl direction. At the end of injection process Spray #1

with a co-swirl direction intersects all sprays of the downstream injector and such interaction sub-zones are shown by a series of black dots.

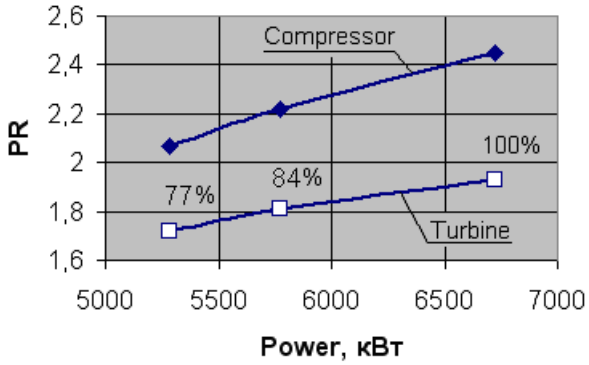


***Figure 9. Turbine and compressor pressure ratio for different operating modes of the engine***.

The negative effect caused by intersection of spays injected by the upstream injector with sprays injected by the downstream one can be significant and usually such the situation is avoided in low speed two stroke marine engines by optimisation of location of several injectors installed around the inlet valve. The mathematical model developed in this work is not yet capable to accurately predict parameters in fuel spray intersection zones but it can be used to determine location and dimensions of fuel injector and parameters of the fuel injection process so to avoid occurrence of intersection zones during the results 3D visualisation stage.

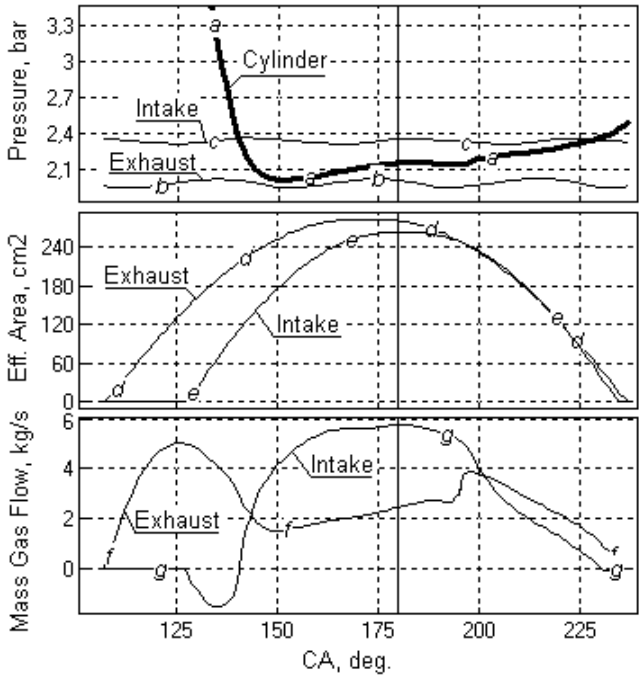


***Figure 10. Parameters of the gas exchange for operating mode in which power output is 77% of the maximum value***

With the increase in the engine power output to 84% and 100% of the maximum value Sprays #1 from both injectors reach the cylinder liner (see Fig. 13) which is unacceptable case since formation of NWF on the cooled cylinder liner results in the increase in the fuel consumption and particulate matter emissions and in diluting lubrication oil by fuel.

Analysis of the obtained data shows a negative trend in the mixture formation with increase in the

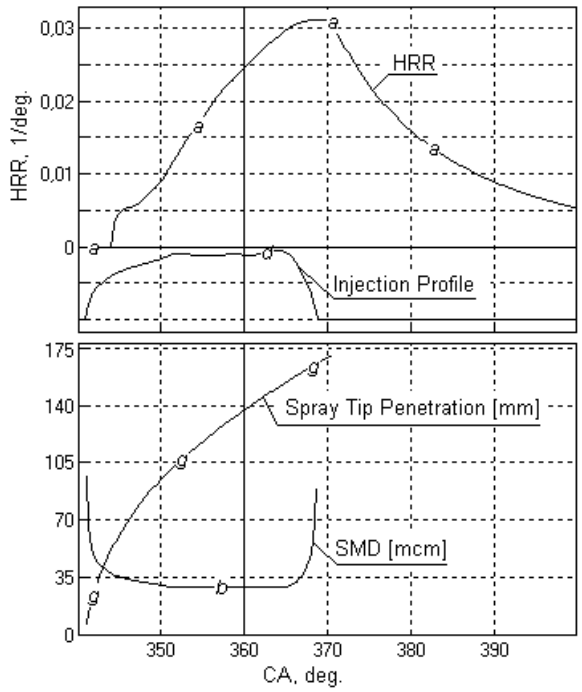


***Figure 11. Parameters of injection process and heat release for operating mode in which power output is 77% of the maximum value***

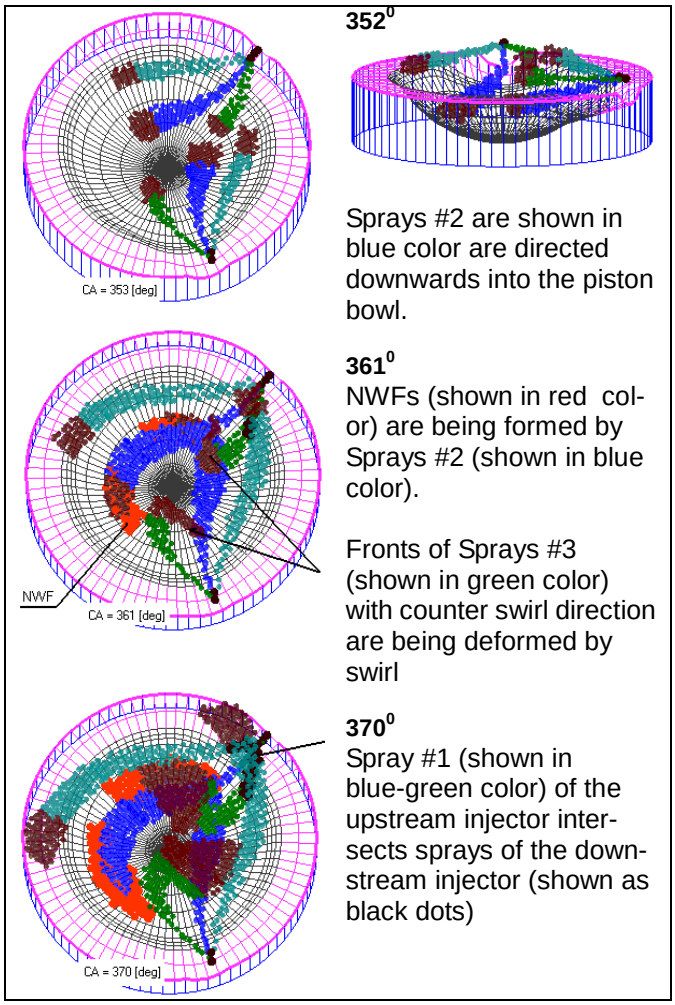


***Figure 12. Evolution of the sprays for the 5152 kW@ 800 RPM operating mode (77%). Fronts of all sprays are shown in brown color***

power output, namely fuel reaches the cylinder liner because of the excessive length of sprays penetration. The solution in this situation is the design of a new fuel system with high injection pressure and larger number

of nozzles. This will reduce the injection time, reduce the sprays penetration length and decrease the diameter of the droplets (as a result of rise of the injection pressure). All these changes will reduce the duration of the combustion process and improve the fuel efficiency. However, it is still necessary to determine new orientation of nozzles to avoid the intersection of fuel sprays and their impingement onto the cylinder liner.

It is also important to monitor the thermal state and resulting thermal loadings in the components of the combustion chamber to maintain their required durability and for the correct simulation of heat transfer in the cylinder of the engine. To calculate the temperature of the piston and cylinder liner a FEM analysis of these parts was conducted, see Fig. 14. It was obtained that for the operating mode with 77% of the maximum power output (5152 kW @ 800 RPM) there was no overheating of components and the maximum temperature was observed on the edge of the piston crown equal to 380 $^0$C.

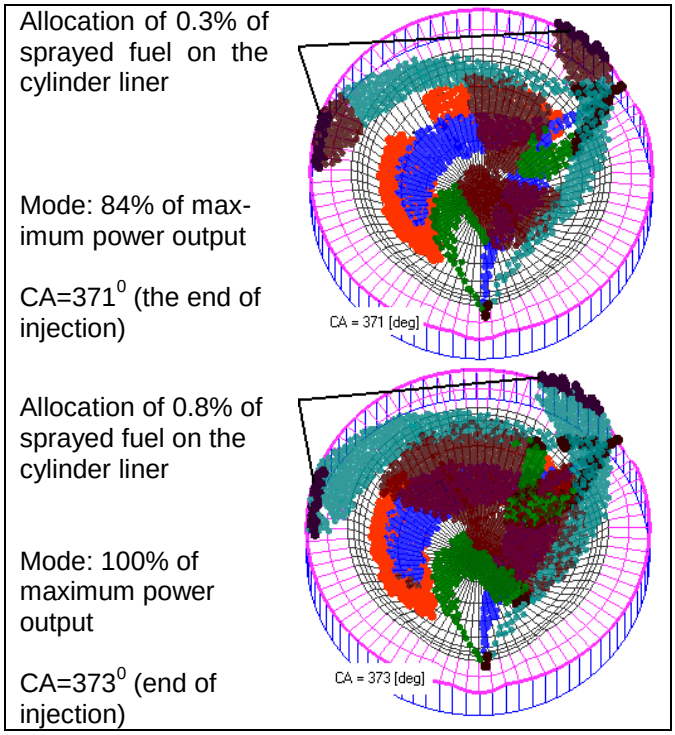


***Figure 13. Geometry of fuel sprays at the end of injection process for the 5667 kW @ 800 RPM (84%) and 6710 kW @ 900 RPM (100%) operating modes***

Simulation results indicate that for operating modes with 84% and 100% of the maximum power output the highest temperature on the piston crown's edge reaches 389 $^0$C and 399 $^0$C, respectively whilst the acceptable value of the temperature for cast iron piston (EN-GJS-600-3) is between 380 and 400 $^0$C.

## OPTIMIZATION OF PARAMETERS OF THE ENGINE WITH INCREASED POWER OUTPUT

The optimization of the engine's parameters along with parameters of a new injection system and injection profiles was performed for operating mode with 120% of the maximum original power output (8000 kW @ 900 RPM). In this optimized design the engine's turbocharger is equipped with a hydraulic coupling to the crank shaft and control system to vary the compressor and turbine pressure ratio (PR). To select optimal values of the PR for the compressor and turbine, the 2D parametrical investigations of these parameters were carried out, see Fig. 15. The optimal point was selected using the following considerations:

- The SFC should be minimal;
- The Air/Fuel equivalence ratio during combustion should be 1.9 or greater;
- Scavenging factor should not be less than 1.27-1.3.

The selected optimal point is labeled by as a black point in Fig. 15.

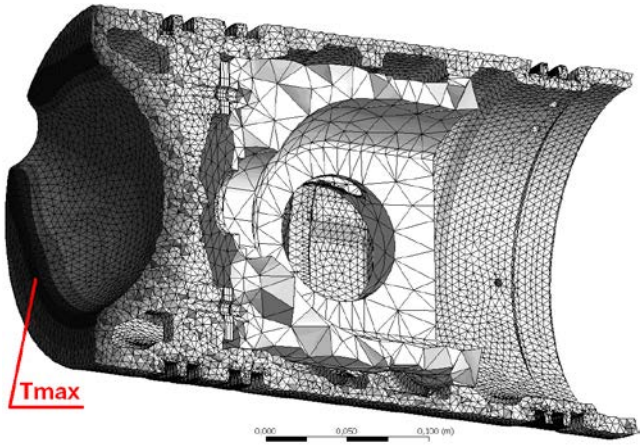


Figure 14. 3D mesh for FEM analysis of the thermal state of the piston using ANSYS software

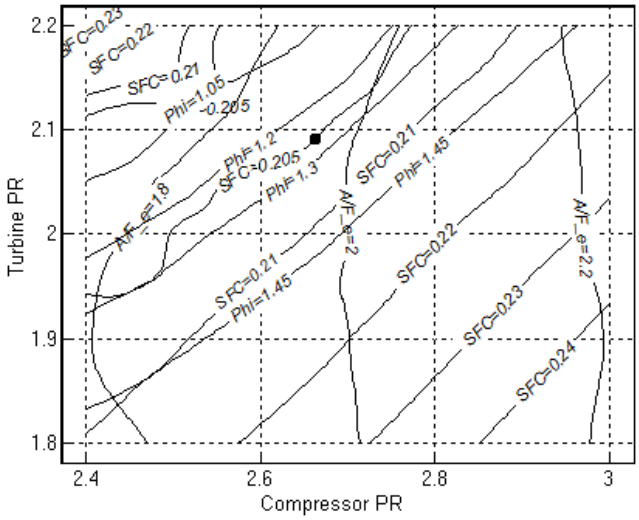


***Figure 15. Effect of Compressor and Turbine PR on engine parameters for the 8000 kW @ 900 RPM operating mode (120% of the maximum original power output)***

Using the above results, a further study was carried out with application of two 4 nozzle sprayers. The additional nozzle #4 with diameter of 0.6 mm is added which is directed into the volume of the cylinder (similar to the adjacent original nozzle #3). The spray from this new nozzle does not impinge onto the bowl of the piston. As a result of a series of numerical experiments on the operating mode with 120% of the original maximum power the best configuration of the fuel spray system was selected as follows (see Table 4):

- Spray #1 is directed slightly upwards to avoid intersection with sprays from another injector during

its evolution. There is no impingement of this spray onto the walls;

- Spray #2 is directed into the piston bowl and forms the large area NWF as a result of impingement;
- Spray #3 has the counter swirl and downwards direction. This spray is rapidly disintegrated by the swirl there is no impingement onto the walls;
- Direction of Spray #4 (shown in yellow color) is very close to that of Spray #3 (there is a very small angle between their axes) Because of its counter swirl direction its core is very short and the large fraction of fuel in this spray is located in its dilute outer zone where evaporation conditions are favorable.

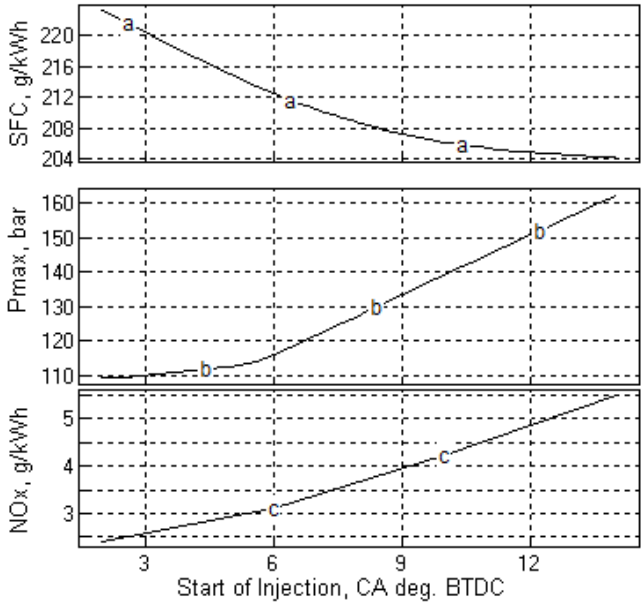


***Figure 16. Effect of Injection Timing on the engine parameters for the 8000 kW @ 900 RPM operating mode (120% of the maximum original power*)**

***Table 4. Specification of the modified injectors***

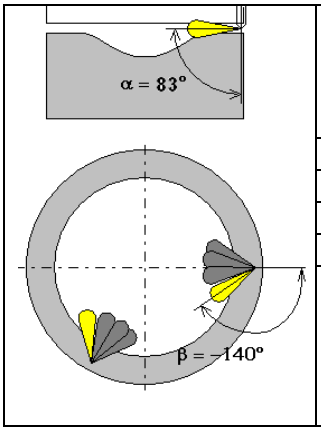


| Nozzles | Bore [mm] $d_n$ | α [deg] | β [deg] |
|---|---|---|---|
| 1 | 0.45 | 96 | 155 |
| 2 | 0.6 | 72.5 | 170 |
| 3 | 0.6 | 80 | -154 |
| 4 | 0.6 | 83 | -140 |

Fig. 17 shows the geometry of sprays obtained as a result of numerical optimization. It can be observed that there are no spatial intersection of sprays and spray/cylinder liner impingements.

The maximum temperature on the edge of the piston crown is now 424$^0$C. It means the original piston or its cooling system must be modified to provide the required piston's durability in the engine with the increased power output.

Parameters of the fuel/air mixture formation and combustion in the engine with optimized working process to operate with 8000 kW power output at 900 RPM are presented in Fig. 18. Results on the SFC of the original and optimized engines are shown in Fig. 19 as a function of power output.

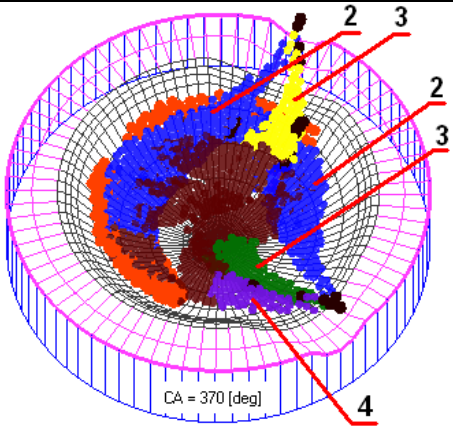


Sprays #1 from both injectors and spray #4 from the furthest injector are not shown. NWF are shown by red. Sprays fronts are marked by brown.

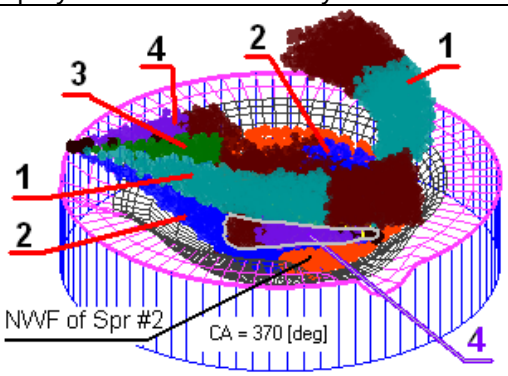


Spray **#4** from downstream injector (highlighted by gray line) develops in the counter swirl direction in the gap formed between spray #1 and spray #2 of the upstream injector.

***Figure 17. Geometry of fuel sprays at the end of injection process for the 8000 kW @ 900 RPM operating mode (120% of the original maximum power output)***

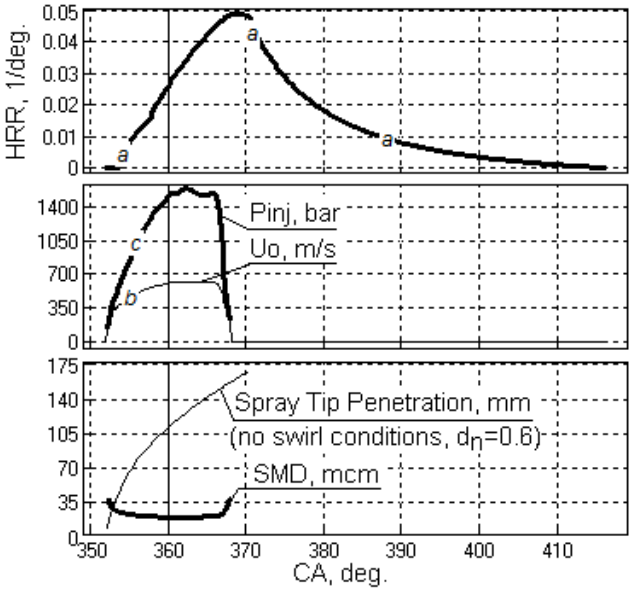


***Figure 18. Parameters of the mixture formation and combustion of the engine with optimized working process to operate with 8000 kW of power output @ 900 RPM***

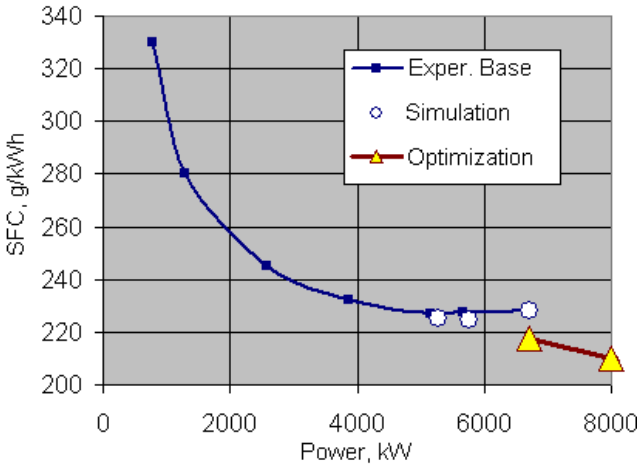


***Figure 19. SFC of the original and optimised engines as function of power output***

Overall, the modified DIESEL-RK can be used for engines optimization research to propose engineering solutions to improve their power output and SFC.

## NUMERICAL ANALYSIS AND DESIGN OF THE ENGINE FUEL INJECTION SYSTEM

Hydrodynamic fuel system simulation tool INJECT has been developed and experimentally validated by one of authors of this article, Prof. L. Grekhov at BMSTU [14-16]. This software has capabilities very similar to those of packages used in industry. In the current research the following specific features of INJECT software were deployed [14,15]:

- Possibility to analyze a fuel system with any arbitrary configuration, see Fig 20;
- Accounting for presence of the vapour phase in liquid fuel during simulations of high pressure (HP) pumps and pipes;
- Accounting for the effect of hydraulic friction in pipelines in conditions of intensive flow unsteadiness;
- Possibility to simulate solenoid actuators and piezoelectric drives of control valves;
- Accounting for variable speed of sound depending on the pressure and temperature of fuel;
- Accounting in the mass balance equations for presence of the vapour or gas phases in fuel;
- Accounting for torsion vibrations in the high pressure pump drives.

To validate INJECT software a series of theoretical and experimental investigations was performed on fuel systems with injection pressure up to 4000 bar. At such high pressure levels diesel fuel is heated due to its compression and whist its flow through orifices. He above factors results in the decrease of the local speed of sound in the sprayer nozzles. At the injection pressure values between 2700 and 2900 bars the adiabatic flow velocity of fuel $U_{ad}$ reaches the local speed of sound $\alpha_s$, see Fig. 21. If the pressure is further increased then the fuel flow velocity $U_{cons}$ reaches its maximum value and then starts to decrease. Thus, the optimal pressure of fuel injection exists diesel engines which is defined not by requirements of low fuel consumption and emission levels but by the fuel flow velocity in the nozzles of injector reaching the speed of sound. This limit in the injection pressure is about 2800 bar and application of injection pressures greater than 2800 bar does not lead to a shorter injection process but increases losses. Consequently, the power required to drive the HP pump considerably increases.

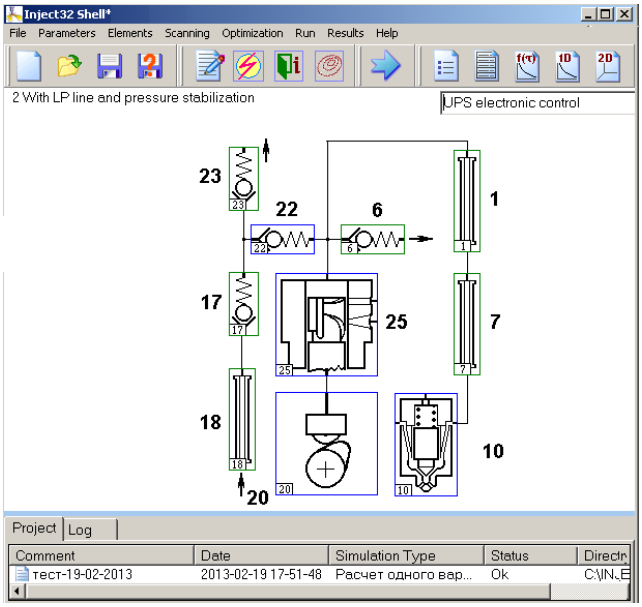


***Figure 20. Illustration of generation of the schematic of an arbitrary fuel system in INJECT software for theoretical analysis and optimization purposes***

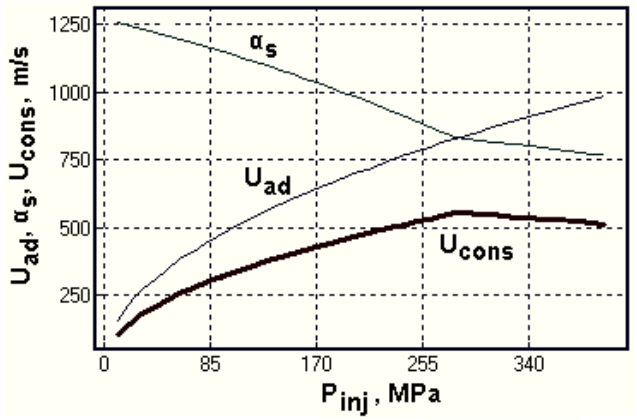


***Figure 21. Adiabatic flow velocity of fuel $U_{ad}$ (a), local speed of sound $\alpha_s$ (b), fuel flow velocity $U_{cons}$ (c) as functions of the injection pressure $p_{inj}$***

SELECTION OF FUEL INJECTION SYSTEM TYPE

Initially, fuel injection profiles were calculated for several operating modes of the original engine with the conventional fuel system design. Results of simulations indicated that the existing fuel system could not satisfy new requirements on providing high injection pressures between 2000 and 2150 bar for greater effective flow areas of nozzles in the new fuel injector (three nozzles with the diameter of 0.6 mm and one nozzle with the diameter of 0.45 mm).

In the second stage a possibility of deployment of various types of new fuel system was considered. The undivided fuel systems (UIS) with electronic control normally are not used in OP engines and would require considerable engine modifications. Systems with multiplication of pressure are too complex in design and their exploitation demonstrated a number of technical

issues.

Two systems which have good prospectives for application in the OP engine are a HP pump with control valve (UPS) and Common Rail System (CRS). A study was conducted on the CRS with the injection pressure 3500 bar. Advantages of the CRS include the precisely controllable injection pressure for different operating modes and relative simplicity of realization of a split multistage fuel injection. From previous study conducted for a locomotive engine on the design of air supply system, EGR and fuel supply systems to satisfy EU Stage IIIB emission regulations it was found that the high injection pressure should be provided across the whole range of the locomotive performance, see Fig. 22 [16]. It can be seen that the UPS does not have a capacity to produce required injection pressure levels even in cases in which complex technical solutions are deployed (e.g. including a stabilizing valve 6 into the scheme shown in Fig. 20). So as a result the CRS only can be used for locomotive applications.

If engine parameters and fuel injection system are optimized for achieving the maximum fuel efficiency then the optimum maximum fuel injection pressure should continuously increase with the rise in power output, see Fig. 23. Thus the UPS has a potential to produce the optimum injection pressure for the medium speed diesel engine if emissions limits are not very demanding.

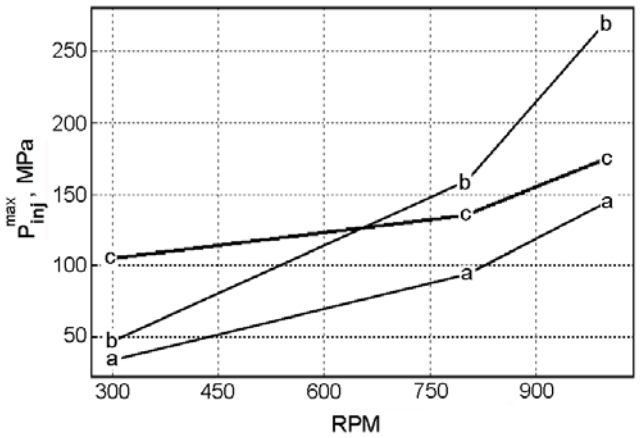


***Figure 22. Maximum injection pressure values for 3 regimes across the locomotive performance range: a, b – produced by UPS; c –required injection pressures to satisfy EU Stage IIIB emission regulations***

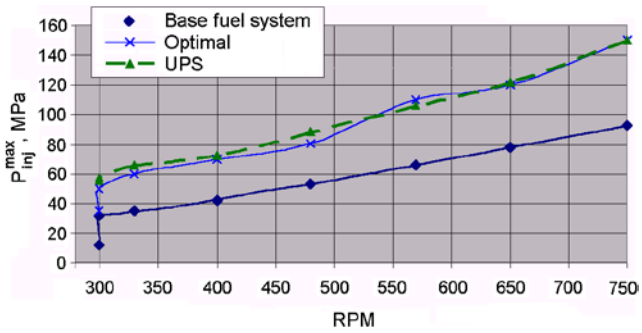


***Figure 23. The maximum injection pressures for achieving the maximum fuel efficiency***

The OP diesel engine, which is the focus of investigations in this work, is not subjected to strict emission restrictions. Therefore there is no need in the precisely controllable injection pressure when changing the mode of operation which makes it possible to exclude the application of the CRS. Taking into account the above outcomes the UPS with a high injection pressure and electronic control is recommended to be used with the OP diesel engine. A high injection pressure at partial loads can be produced by overall high intensity of the fuel supply and by incorporating additional technical modifications (e.g. including into the design a stabilizing valve).

There are two potential options with application of the UPS: the first is using a single HP pump for two injectors; the second option is using two HP pumps per cylinder with one HP pump for each injector (see Table 5). Comparison of these options is presented in Table 6. In the original OP engine the second option is deployed, namely using two HP pumps per cylinder.

***Table 5. Specifications of two UPS options***

| Pump per cylinder | $m_f$ g | RPM | $\mu F_{noz}$ $mm^2$ | $d_{pl}$ mm | $h_{pl}$ mm | $P_{inj}^{max}$ bar |
|---|---|---|---|---|---|---|
| 1 | 2.34 | 900 | 1.35 | 22 | 30 | 2250 |
| 2 | 1.17 | 900 | 0.67 | 17 | 24 | 2100 |

***Table 6. Comparison of to UPS options***

| Using one HP pump per cylinder | Using two HP pumps per cylinder |
|---|---|
| - Lower price;<br>- Improved reliability due to reduced number of parts. | - Reduced price per HP pump due to greater volume of production;<br>- Lower load on plunger actuators at high injection pressures;<br>- Improved reliability of the diesel engine and survivability of the vessel (when one the fuel pumps fails);<br>- Lower fuel consumption when operating at the partial load (only one of HP pumps can be used);<br>- Improved control of characteristics and injection pressure. |

NUMERICAL OPTIMIZATION OF FUEL INJECTION SYSTEM

The following are requirements for the performance of fuel supply system for the OP engine:

- Injection pressure should not be less than 2000 bar;
- Injection timing should be controllable;
- The optimum shape of the fuel injection profile should be precisely achieved;
- The possibility of the rapid termination of the fuel injection should be provided;
- The stabilization of the plunger volume filling should be achieved.

The injection pressure increase is achieved in several different ways. During development of the design of the new fuel pump different shapes of cams were considered and the concave cam with the radius

of the base circle of 48 mm was selected, see Fig. 25. Such the design provides the maximum speed of the plunger of 4 m/s, the duration of the constant speed of 24 degrees, the injection pressure of 2010 bar at the maximum cam surface stress being 1937 MPa.

The option, in which two HP pumps per one cylinder are used, demonstrates a better performance with the maximum speed of the plunger being 3.05 m/s, the duration of the constant speed being 33.2 degrees, the injection pressure being 2090 bar at the maximum cam surface stress equal to 1512 MPa.

Reducing the dead volume of each pump from 6850 $mm^3$ down to 1400-1700 $mm^3$ increases the maximum injection pressure by 33 MPa, see Fig. 26.

The injector was completely redesigned in accordance with the above requirements to achieve an improved operational capability at high thermal loads. However, connecting parts and their dimensions and interchangeability with the base injector was preserved. In the new injector the following parameters were reduced: mass of moving parts (by factor of 3.5), the internal volume (by factor of 2) and the suction volume (by factor of 10). The injector in the new system was equipped with the additional nozzle.

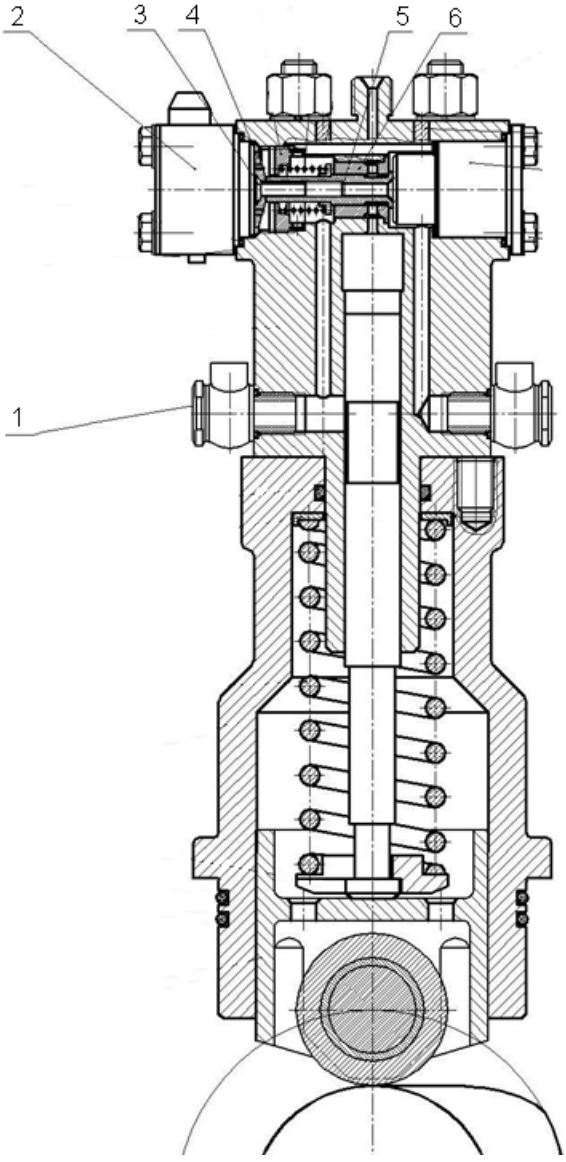


***Figure 24. 22x30 mm HP pump with the electronic control and fuel delivery into two injectors: 1 – output fitting; 2 – solenoid actuator, 3 – screw; 4 – armature; 5 – control valve; 6 – valve barrel.***

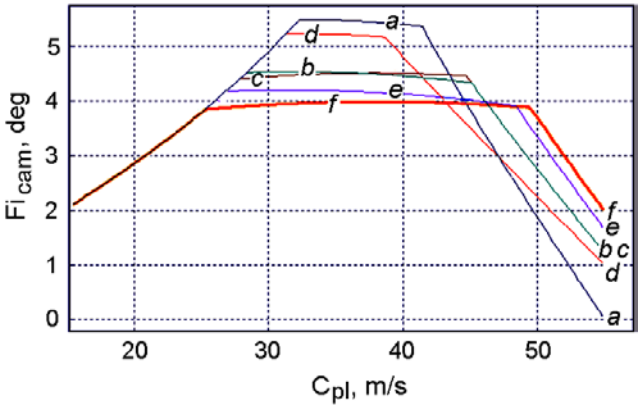


***Figure 25. Plunger speed as a function of the cam angle for different cam profiles (a - f) with the radius of the base circle of 48 mm. The variant f is selected for further use.***

The new injector parameters are optimized for the large injection pressure and rapid closing speed of the needle. The high precision surface of the needle was placed away from the suction volume of the hot sprayer. A needle with the diameter of 6 mm and the lift of 0,38 mm is used. The new injector increases the injection pressure by 22-24 MPa.

The designing experience of the UPS demonstrated that a special attention was required when designing the Low Pressure Line (LPL), see Fig. 25, since heated fuel with a significant vapor phase may form and remain in the volume 6 of the control valve 5 after the filing process. During the next intake of fuel into the plunger volume through the valve 5 this vapour phase causes the incomplete filling of the volume resulting in the poor performance of the pump, delay of injection start and cyclic fuel mass instability.

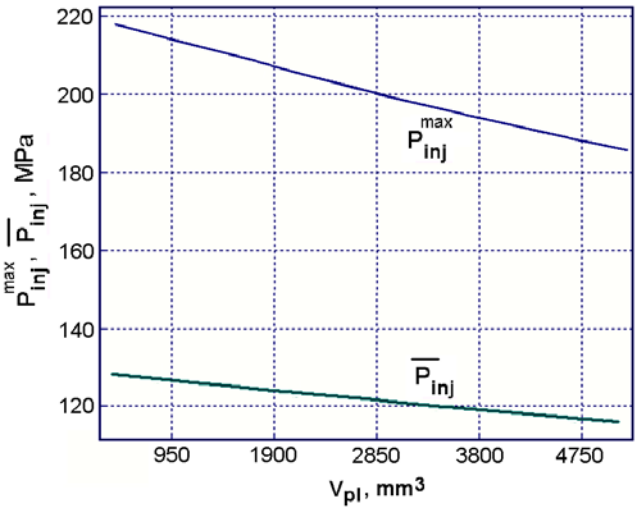


***Figure 26. Injection pressures (maximum (a) and average (b)) as functions of dead volume in the HP pump***

The guaranteed circulation of fuel through the LPL and timely removal of the hot vapour containing fuel from the control valve require application of pipelines with the inner diameter of 8 mm and the back-flow valve 10, see Fig. 27. In a simpler version of the LPL there are two orifices can be installed, namely the inlet and outlet orifices. The effective flow area of the inlet orifice is $\mu F_7$ = 5 -7 $mm^2$, and the effective flow area of the outlet orifice should be $\mu F_{10}$ >15-18 $mm^2$, see Fig. 28.

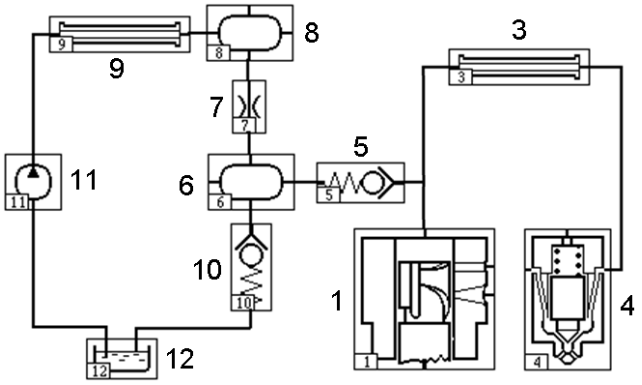


***Figure 27. Calculation scheme for analysis of the Low Pressure Line for the fuel supply to the control valve 5.***

For intensification of the fuel injection the diameter of the delivery pipe was optimized using equations derived using experimental results in [16] for the determination of the unsteady hydrodynamic friction in pipes. The optimized diameter of the delivery pipe is 2.5 mm

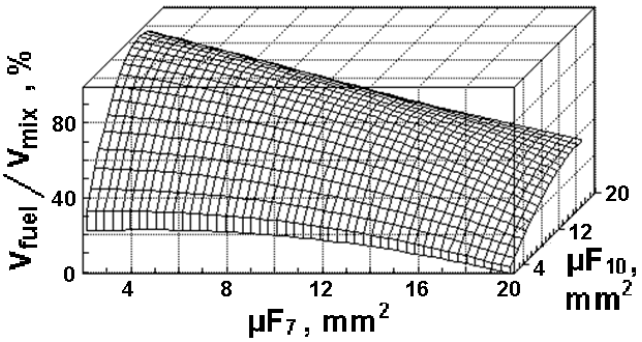


***Figure 28. Volumetric efficiency of the plunger volume as a function of the effective flow area of the input ($\mu F_7$) and outlet ($\mu F_{10}$) orifices***

## CONTROL VALVE OPTIMIZATION

The effective flow area of the control valve should provide a sharp rise in the injected fuel flow and its sharp decrease in accordance with the injection profile. In theory, for the current case, for the valve with the diameter of 12 mm the valve's stroke 0.25 ÷ 0.3 mm was sufficient. However, the different valve's stroke was needed for the perfect filling of the plunger cavity without the formation of the gas phase. Figure 29 shows the formation of the considerable amount of gas in the plunger cavity during the suction through the open control valve. Formation of the most of gas takes place when the velocity of the plunger is reducing. There are two criteria for definition of the perfect filling: the first is more stringent criterion and limits the maximum volume of formed gas; the second criterion is less strict and related to the gas content at the end of the filling process. To satisfy both criteria on the quality of the filling and injection processes the valve stroke of 0.4 mm and the feeding pressure of 1.0 MPa were selected

Another important parameter of the control valves of this type (see Fig. 30) is their pressure-compensation.

When the fuel flows through the control valve the distribution of the static pressure on the valve's surface varies and the hydraulic pressure compensation of the valve becomes unbalanced. To analyze this phenomenon a mathematical model for rapid simulations

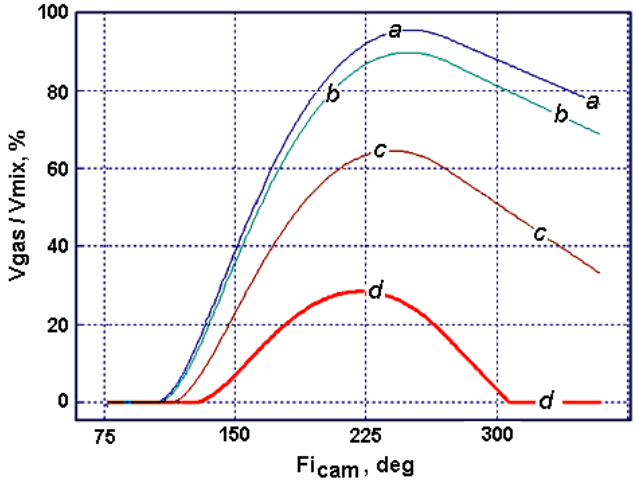


***Figure 29. The volume ratio of gas during the filling of the plunger cavity: a – the valve lift is 0.25 mm and feeding pressure is 0.3 MPa, d – the valve lift is 0.4 mm and the feeding pressure Is 0.6 MPa***

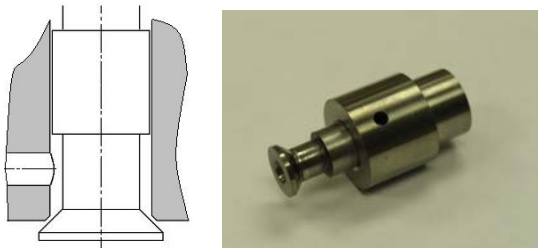

***Figure 30. The schematic and appearance of the pressure-compensated control valve***

of the fuel flow was developed taking into account the local hydraulic losses. The empirical coefficients for this model were obtained during special experiments and equation was derived to calculate the discharge coefficient $\mu_{val}$ for a typical valve unit:

$$\mu_{\text{val}} = 0.8 - 2.2686\left(\frac{h_{\text{val}}}{d_{\text{val}}}\right)^{0.533},$$

where $\mu_{val}$ corresponds to the minimum flow area of the valve gap; $h_{val}$ is the valve stroke; $d_{val}$ is the discharging plunger diameter of valve.

## SOLENOID ACTUIATOR OPTIMIZATION

Optimization of dimensions, materials and deployment of complex control algorithms made it possible to minimize the size of the electromagnetic actuator and limit its force to 150 N.

The use of composite materials for the magnetic circuit reduced eddy currents and the coercive force (determined by the width of the hysteresis diagram). Preliminary powering of the solenoid actuator (prior to the peak impulse) accelerated the process of achieving the magnetic saturation induction. Both these measures reduced the response time of the electromagnet down to 0.1 ms (by 25%).

The OP engine operation requires a split multi-stage fuel injection. Therefore, the developed system was tested for its capacity to provide double stage fuel injection in partial load regimes, see Fig. 31. The multi-stage injection is not required for the full load regime of operation. The modifications which were introduced

(minimizing the volumes of the HPL, dimensions of the delivery pipeline, reducing the solenoid actuator response time, reduction of the moving masses) resulted in possibility to carry out multistage fuel injection in accordance with the required specifications: the pilot portion does not exceed 4% of the cyclic fuel mass and the guaranteed interval between stages of injections does not exceed 0.27 ms.

The developed UPS provides a continuous rise in the injected fuel mass with increasing the duration of the controlling signal which is beneficial for the OP engine operation.

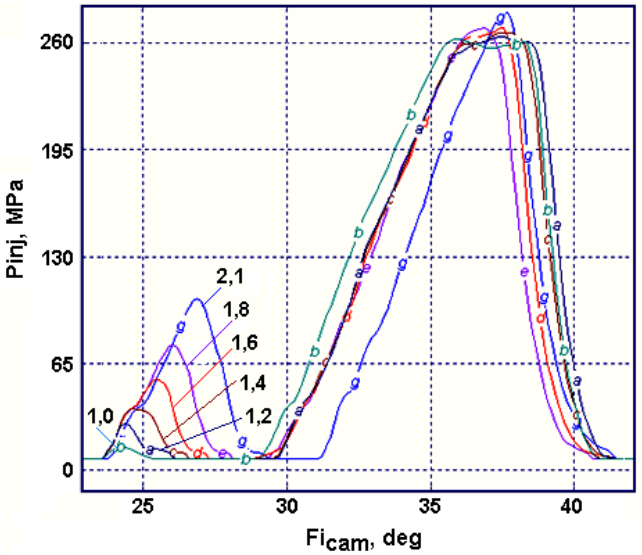


***Figure 31. Injection pressure profiles for multi-stage fuel injection for different durations of the pilot injection (1-2.1 ms)***

## CONCLUSIONS

1. The mathematical model for rapid numerical simulations and calculation of parameters of gas, vapour and liquid fuel droplets was developed which allows to predict variation of the pressure and temperature in the engine cylinder and select the configuration and design of fuel injectors for realization of the improved fuel/air mixing process.
2. Optimisation of working cycle and design parameters of the mid speed OP diesel engine was carried out to increase its original maximum power output by 20% and reduction of its Specific Fuel Consumption.
3. It was found that in the engine with its original fuel injectors fuel spray/cylinder liner impingements took place at increased loads causing the rise in particulate matter emissions and diluting of lubrication oil with fuel. Additionally, the fuel spray from the co-swirl directed nozzle of the upstream fuel injector intersected all fuel sprays of the downstream fuel injector causing deterioration in their evaporation. A relatively low pressure of fuel injection in original injectors does not provide fine fuel atomization and prolongs the period of injection process.
4. The new fuel injection system designed in this work makes it possible to increase the original maximum power output up to 8000 kW. The elimination of spatial intersections of sprays and fuel spray/cylinder liner impingements resulted in the improved engine fuel conversion efficiency.
5. Overheating of the cast iron piston of the engine is a limiting factor in increasing the engine's power output. New design of the piston and its cooling arrangements should be provided in the new engine.
6. If strict emission restrictions are not imposed on the operation of the medium speed OP diesel engine then application of the UPS is a feasible option. The newly designed UPS fully satisfies requirements for the efficient diesel operation with power output 6700-8000 kW @ 900 RPM. The maximum injection pressure of the newly designed UPS is about 200 MPa.
7. One of the components of the HP pump, namely the control valve with solenoid actuator, requires careful design optimization to ensure the pressure-compensation of the valve during the fuel flow. Additionally, optimization of the transient electromagnetic processes in the high-speed solenoid actuator is required.
8. Optimization of the plunger cavity filling process and of the low pressure line is required to ensure the stability of the fuel injection process.

## ACKNOWLEDGMENTS

This research is supported by EU Marie-Curie International Incoming Fellowship Grant FP7-PEOPLE-2012-IIF/PIIF-GA-2012-328361.

Authors would like to acknowledge support of JSC Production Association "Diesel-Energo" and providing the engine experimental data.

Special thanks Drs Philipp Barchenko and Nikolay Malastovski for FEM analysis of the thermal state of the engine parts in this project and to Alexey Kuleshov for developing software for 3D visualisation of the fuel sprays evolution in the engine's cylinder.

## REFERENCES

1. L. Fromm, R. Herold, J. Koszewnik, G. Regner, "Modernizing the opposed-piston engines for more efficient military ground vehicle applications" // 2012 NDIA Ground Vehicle Systems Engineering and Technology Symposium / Power and Mobility (P&M) Mini-Symposium, August 14-16, Michigan. – 9 p.

2. Jean-Pierre Pirault, Martin Flint, "Opposed Piston Engines: Evolution, Use, and Future Applications." SAE International, Warrendale, Pa, ISBN 978-0-7680-1800-4, 2009.- 563 p.

3. Riazancev N.K., Modern Ukrainian tank diesels // Dvigatelestroenie. – 2001. – No 3. – p. 3-5. (In Russian).

4. Kinzhalov O.S. Diesels and gas engines. Branch catalogue. Moscow, 1991, 192 p. (in Russian).

5. A.S. Kuleshov, "Model for predicting air-fuel mixing, combustion and emissions in DI diesel engines over whole operating range," SAE Tech. Pap. Ser. 2005-01-2119, 2005.

6. A.S. Kuleshov, "Multi-Zone DI Diesel Spray Combustion Model for Thermodynamic Simulation of Engine with PCCI and High EGR Level," SAE Tech. Pap. Ser. 2009-01-1956, 2009.

7. A.S. Kuleshov, A.V. Kozlov, K. Mahkamov, "Self-Ignition Delay Prediction in PCCI Direct Injection Diesel Engines Using Multi-Zone Spray Combustion Model and Detailed Chemistry," SAE Tech. Pap. Ser. 2010-01-1960, 2010.

8. Kuleshov A.S. "Multi-Zone DI Diesel Spray

Combustion Model and its application for Matching the Injector Design with Piston Bowl Shape" SAE Tech. Pap. Ser. 2007-01-1908, 2007.

9. Kuleshov A.S. "Development of simulation methods and optimization of working processes of ICE" Autoref. Diss. Doct. Tech. Sc. - Moscow, 2011. (in Russian)

10. Razleytsev, N.F., 1980, "Combustion simulation and optimization in diesels", Kharkov: Vischa shkola, 169 p. (In Russian).

11. Lyshevsky, A.S., 1971, "Fuel atomization in marine diesels," Leningrad, 248 p. (In Russian).

12. Vyrubov, D.N., 1954, "Method of calculation of fuel evaporation," Publications of BMSTU, Vol. 25, pp. 20-34. . (In Russian)

13. Vyrubov, D.N., 1946, "Formation of air/fuel mixture in IC engines. In "Working processes of IC engines", Moscow, MASHGIZ, pp. 5-54. (In Russian).

14.http://energy.power.bmstu.ru/e02/inject/i03rus.htm

15. Grekhov L.V., Gabitov I.I., Negovora A.V. Design, calculation and technical service of fuel equipment of modern diesel engines: Textbook. - M .: Publishing House of the Legion Autodata, 2013. - 292 p. (In Russian).

16. Kuleshov A.S., Grekhov L.V. Multidimensional Optimization of DI Diesel Engine Process Using Multi-Zone Fuel Spray Combustion Model and Detailed Chemistry NOx Formation Model", SAE Tech. Pap. Ser. 2013-01-0882, 2013.

## CONTACTS

Dr. Sc (Tech), Professors:
Leonid Grekhov (lgrekhov@mail.ru) and
Andrey Kuleshov
(andrei.kuleshov@northumbria.ac.uk)

## DEFINITIONS, ACRONYMS, ABBREVIATIONS

| | |
|---|---|
| $A_{actual}$ | Actual area filled with liquid at the Injector Exit Cross-Section, $m^2$ |
| $A_{theor}$ | Theoretical (geometrical) area of Cross-Section at the Injector Exit, $m^2$ |
| **BMEP** | Break Mean Effective pressure |
| **BSFC** | Break Specific Fuel Consumption |
| **CRS** | Common Rail System |
| $d_{val}$ | Discharging plunger valve diameter |
| $d_{pl}$ | Plunger diameter of HP pump |
| **HP pump** | High Pressure pump |
| **HPL** | High Pressure Line |
| **HRR** | Heat Release Rate |
| $h_{val}$ , $h_{pl}$ | Valve stroke, plunger stroke |
| **LPL** | Low Pressure Line |
| $m_f$ | Cyclic fuel mass |
| $n$ | Engine speed (cam speed) |
| **NWF** | Near Wall Flow of fuel droplets/air mixture spreading along the wall |
| **OP** | Opposed Piston |
| $P_{inj}$ | Injection pressure |
| $P_{inj}^{max}$ | Maximum injection pressure |
| $\overline{P}_{inj}$ | Average injection pressure |
| **PR** | Pressure Ratio |
| **SFC** | Specific Fuel Consumption |
| **SMD** | Sauter Mean Diameter of droplets $d_{32}$ |
| $U_{ad}$ | Fuel adiabatic flow velocity |
| $U_{cons}$ | Average velocity for the calculation of fuel consumption through the spray hole |
| **UPS** | Unit Pump System (divided fuel system) |
| **UIS** | Unit Injector System (undivided fuel system) |
| $\alpha_s$ | Local speed of sound |
| $\mu F$ | Effective cross-section area |
| $\mu_{val}$ | Valve flow coefficient |

## APPENDIX A

Integral parameters of the original engine

| | 5152 kW@ 800 RPM (77%) | | | 5667 kW @ 800 RPM (84%) | | | 6710 kW @ 900 RPM (100%) | | |
|---|---|---|---|---|---|---|---|---|---|
| | Exper. | Simul. | Δ% | Exper. | Simul. | Δ% | Exper. | Simul. | Δ% |
| Power, kW | 5152 | 5178 | -0.5 | 5667 | 5746 | -1.4 | 6710 | 6672 | 0.6 |
| SFC, g/kWh | 226.8 | 225.6 | 0.5 | 227.6 | 224.6 | 1.3 | 228 | 229.3 | -0.6 |
| P max, bar | 114 | 110 | 3.5 | 118 | 116.3 | 1.4 | 130 | 127 | 2.3 |
| T before turbine, K | 690 | 755 | -9.4 | 720 | 752 | -4.4 | 735 | 752 | -2.3 |
| Mass air flow, kg/s | 13.1 | 12.3 | 6.1 | 14.4 | 13.8 | 4.2 | 16.9 | 16.62 | 1.7 |